Experimental Realization of Nonreciprocal Adiabatic Transfer of Phonons in a Dynamically Modulated Nanomechanical Topological Insulator

Tian Tian,[1,2] Yichuan Zhang,[1,2] Liang Zhang,[1,2] Longhao Wu,[1,2] Shaochun Lin,[1,2] Jingwei Zhou,[1,2,*] Chang-Kui Duan,[1,2] Jian-Hua Jiang,[3] and Jiangfeng Du[1,2,4,†]

[1]*CAS Key Laboratory of Microscale Magnetic Resonance and School of Physical Sciences, University of Science and Technology of China, Hefei 230026, China*

[2]*CAS Center for Excellence in Quantum Information and Quantum Physics, University of Science and Technology of China, Hefei 230026, China*

[3]*Institute of Theoretical and Applied Physics, School of Physical Science and Technology and Collaborative Innovation Center of Suzhou Nano Science and Technology, Soochow University, Suzhou 215006, China*

[4]*Hefei National Laboratory, University of Science and Technology of China, Hefei 230088, China*

(Received 8 June 2022; revised 31 August 2022; accepted 28 October 2022; published 18 November 2022)

High quality nanomechanical oscillators are promising platforms for quantum entanglement and quantum technology with phonons. Realizing coherent transfer of phonons between distant oscillators is a key challenge in phononic quantum information processing. Here, we report on the realization of robust unidirectional adiabatic pumping of phonons in a parametrically coupled nanomechanical system engineered as a one-dimensional phononic topological insulator. By exploiting three nearly degenerate local modes—two edge states and an interface state between them—and the dynamic modulation of their mutual couplings, we achieve nonreciprocal adiabatic transfer of phononic excitations from one edge to the other with near unit fidelity. We further demonstrate the robustness of such adiabatic transfer of phonons in the presence of various noises in the control signals. Our experiment paves the way toward nonreciprocal phonon dynamics via adiabatic pumping and is valuable for phononic quantum information processing.

DOI: 10.1103/PhysRevLett.129.215901

Introduction.—Manipulating phonon propagation in nanomechanical systems can lead to cutting-edge applications such as imaging sensing [1,2], phononic switch [3,4], phononic logic gate [5,6], and nonreciprocal phononic devices [7–9]. In the past years, remarkable progress in nanomechanical systems including nonclassical mechanical states [10,11], high-quality oscillators [12–14], and hybrid quantum devices [15,16] have made them an ideal platform for phononic quantum information processing. However, until now, coherent transfer of phonons between distant nanomechanical oscillators with no direct coupling, which is crucial for scalable phononic quantum technology, remains a challenge in experiments, although phononic dynamics in a few mechanical modes have been observed [17–24].

A common approach toward such a goal is to use swap operations between two phononic modes [17–21]. In an array of coupled nanomechanical oscillators, such an approach requires a series of gate operations with fine-tuned interactions and is therefore highly challenging. Another protocol is the perfect coherent transfer [25,26] which is a reciprocal scheme where the fine-tuned intersite couplings lead to the coherent transfer of the initial excitations in a mirror-symmetric way. Although realized in a few experimental systems [27–32], this scheme too depends on the precise control of the fine-tuned couplings as well as the accurate timing of the dynamics and is thus neither robust nor scalable.

On the other hand, inspired by recent developments in topological acoustics and topological mechanics in macroscopic systems [33–43], the study of topological nanomechanical oscillator systems which is at the interface between topological physics and on-chip phononic technology have gained lots of interest [44–46].

Here, we report on the realization of robust, nonreciprocal coherent transfer of phonons across an array of parametrically coupled nanomechanical oscillators via a scheme of adiabatic pumping. The scheme is based on the dynamically modulated one-dimensional (1D) Su-Schrieffer-Heeger (SSH) model [47–56] and is suggested to be superior, i.e., faster, scalable, higher fidelity, and more robust against nonadiabatic effects, than the known Thouless and other topological pumping schemes [49,50]. With such a scheme, the initial phononic state can be efficiently transferred to the targeted oscillator in the forward direction, where the backward propagation is suppressed. We further confirm the robustness of the scheme by adding various noises to the electrical control of the couplings between the oscillators. These discoveries demonstrate that dynamically modulated topological phononic systems offer a new route toward robust, nonreciprocal coherent phonon transfer. Our Letter opens a pathway toward adiabatic nonreciprocal phonon

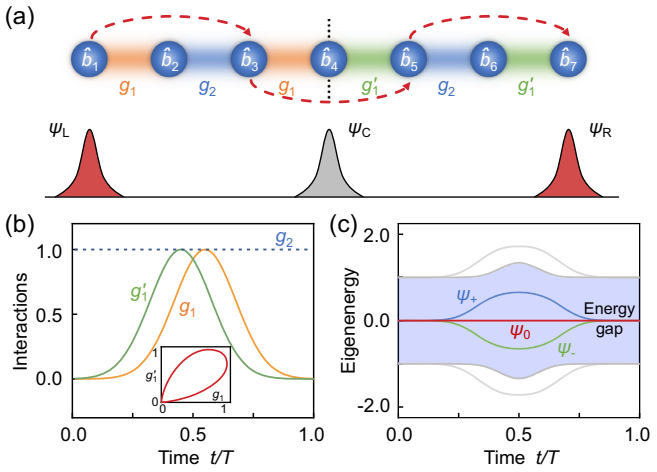

FIG. 1. Schematic of phonon transfer in a Gaussian-modulated topological insulator. (a) The 1D SSH topological insulator with an interface defect. The black dashed line indicates the interface between two standard SSH chains. The staggered couplings of two topological chains are g_1, g_2 and g_1', g_2. This structure with large enough sites has three local states $|\psi_{L,C,R}\rangle$. Red arrows represent the transmission path in an array of phonon cavities (blue balls) via the topological zero-energy state $|\psi_0\rangle$. (b) The time-dependent interactions $g_1(t)$ and $g_1'(t)$ with Gaussian form while the interaction g_2 remains unchanged in the topological structure. The inset exhibits the trajectory in the space (g_1, g_1'). (c) Eigenenergy spectrum of the Gaussian-modulated topological insulator with $N = 7$. Gray lines stand for the upper and the lower energy bands. Three localized eigenmodes appear at the energy gap shown by the blue area.

dynamics and quantum state transfer, and is valuable for future quantum technology based on integrated phononic systems.

Gaussian-modulated topological insulator.—As shown in Fig. 1(a), we consider a 1D phononic topological insulator made of an array of $N = 2M - 1$ ($M \in$ even) phonon cavities. Specifically, this topological insulator includes two standard SSH chains combined by an interface site. Both the first SSH chain with staggered couplings $g_1 < g_2$ and the second chain with staggered interactions $g_1' < g_2$ are topological nontrivial and each chain has two edge localized states [56]. Due to the sublattice symmetry, these local modes appear at the energy gap of the SSH insulator. Therefore, the structure of Fig. 1(a) supports three nearly degenerate local modes: two edge modes and an interface mode between the two SSH chains. The shape of wave functions $|\psi_{L,C,R}\rangle$ of these local modes and their mutual couplings depend on the parameters $\epsilon = -g_1/g_2$ and $\eta = -g_1'/g_2$ [57]. By dynamically modulating g_1 and g_1' while keeping g_2 fixed, theories predict that it is possible to realize adiabatic pumping among these three states that are lying in the topological band gap of the SSH model [49,50]. The advantage of this scheme is that the topological band gap protects these three states and the adiabatic pumping, making them robust against imperfection, noises and nonadiabatic effects.

To achieve the adiabatic pumping, we choose the following Gaussian modulations: $g_1(t) = G_0 \exp[-(t - \delta/2 - T/2)^2/w^2]$ and $g_1'(t) = G_0 \exp[-(t + \delta/2 - T/2)^2/w^2]$ with delay $\delta > 0$, while $g_2 = G_0$ is fixed during the entire pumping process $0 < t < T$ [Fig. 1(b)]. Such dynamic modulations break the time-reversal symmetry and induce the nonreciprocal adiabatic pumping [58,59]. Due to the interaction and hybridization of $|\psi_L\rangle$, $|\psi_R\rangle$ and $|\psi_C\rangle$, the three localized states of a finite system is represented as $|\psi_0\rangle$ and $|\psi_\pm\rangle$. Figure 1(c) gives the eigenenergy spectrum of $N = 7$ which shows that the three localized states are preserved and protected within the topological band gap (the blue region) during the whole pumping process which is a key difference between the Thouless pumping. Such protection gives rise to the robustness of the adiabatic pumping studied here.

The zero-energy state of a long but finite system can be described by the linear combination of $|\psi_{L,C,R}\rangle$ as

$$|\psi_0\rangle \simeq \frac{C_R}{\sqrt{C_L^2 + C_R^2}}|\psi_L\rangle - \frac{C_L}{\sqrt{C_L^2 + C_R^2}}|\psi_R\rangle. \quad (1)$$

Here, $C_L = f_L(M, \epsilon, \eta)g_1$ and $C_R = f_R(M, \epsilon, \eta)g_1'$ where f_L and f_R are two functions depending on the system size [57]. The delay between $g_1(t)$ and $g_1'(t)$ ensures that at $t = 0$ $g_1' \gg g_1$ and hence $C_R \gg C_L$ and $|\psi_0\rangle \to |\psi_L\rangle$, whereas at $t = T$ $g_1 \gg g_1'$ and hence $C_L \gg C_R$ and $|\psi_0\rangle \to -|\psi_R\rangle$. Therefore, through the adiabatic pumping, the initial state $|\psi_L\rangle$ is converted to the final state $|\psi_R\rangle$ [49]. The adiabatic condition here is $\int_0^T dt\sqrt{C_L^2 + C_R^2} \gg \pi/2$ [49]. As the adiabatic pumping is mainly relevant to the three localized states within the band gap, it resembles the stimulated Raman adiabatic passage [49,50,57,60]. Careful analytical and numerical study of the adiabatic pumping is presented in detail in the Supplemental Material [57].

Experimental setup.—In the experiment, we fabricate an array of doubly clamped nanomechanical oscillators of high-stress silicon nitride on a silicon substrate [Fig. 2(a)]. Benefited from the top gold layer (~10 nm) and the phonon frequency differences (see Supplemental Material [57]), we can realize tunable electrostatic interactions between adjacent oscillators [44,61]. With the staggered couplings depicted in Fig. 1(a), seven nanomechanical oscillators form a finite 1D phononic SSH system.

To quantify the coupling between the oscillators, we measure the frequency response spectrum of the fifth oscillator from a lock-in amplifier by the magnetomotive driving and detection technique [62]. The coupling strength g is determined by the spectrum split in Fig. 2(b). Importantly, the coupling g_4 scales linearly with the amplitude $V_{\rm pk}^{45}$ of parametric voltage when the frequency difference $\Omega_4 - \Omega_5$ remains unchanged. This technique is applied to realize other parametric couplings between the oscillators. Taking into account of these couplings, the

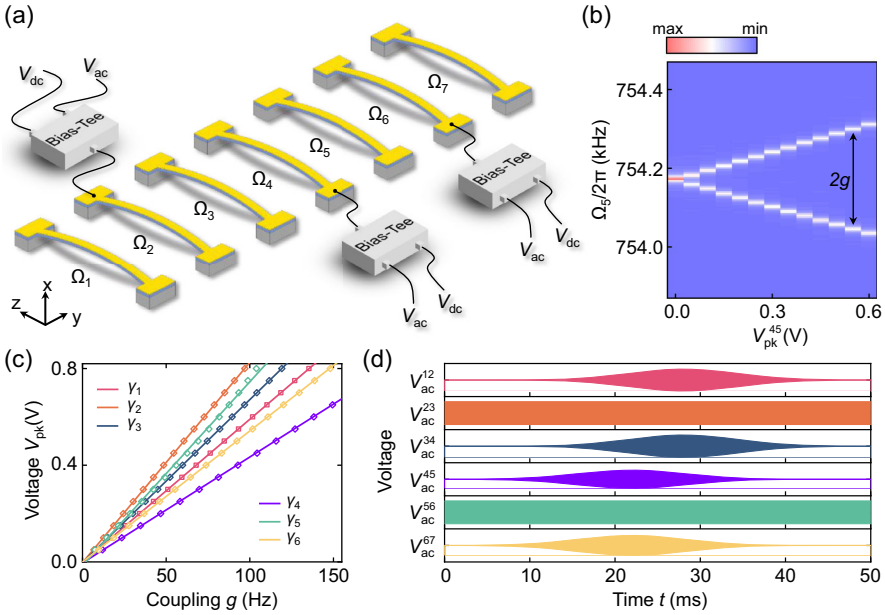

FIG. 2. Dynamically modulated nanomechanical topological insulator. (a) Experimental setup. An interaction of adjacent oscillators is fully controlled by the voltage $V_{ac}^{ij}(t) = V_{pk}^{ij}\cos[(\Omega_i - \Omega_j)t]$ with a fixed dc voltage V_{dc}. The ac voltage and dc voltage are combined via a Bias-Tee in the experiment. (b) The tunable parametric coupling between fourth and fifth oscillators under $V_{dc} = 9.5$ V. (c) Experimental results of the linear relationship between voltage amplitude V_{pk} and coupling g for six parametric couplings under $V_{dc} = 9.5$ V. The slope γ_i is obtained by fitting experimental data. (d) All ac voltages are shaped to realize the Gaussian-modulated topological insulator with the transmission period $T = 50$ ms, the width $w = 9$ ms and the delay constant $\delta = 6.1$ ms.

effective phononic Hamiltonian in the system can be expressed within the rotating wave approximation as [63]

$$\hat{H}_{\text{eff}} = \sum_{i}^{N-1} g_i(\hat{b}_i^\dagger \hat{b}_{i+1} + \hat{b}_{i+1}^\dagger \hat{b}_i), \tag{2}$$

where $\hat{b}_i$ is the annihilation operator of the ith phononic cavity, g_i denotes the coupling between the ith and $(i+1)$th oscillators. The tunability of these couplings are confirmed by careful experimental calibration of the frequency splittings in Fig. 2(c). By varying parametric voltages V_{pk}^{ij} in time domain according to these fitting slopes γ_i in Fig. 2(c), Gaussian-modulated interactions $g_1(t)$ and $g_1'(t)$ are realized and a dynamically modulated phononic insulator is implemented.

Nonreciprocal adiabatic pumping of phonons.—To realize efficient adiabatic phonon pumping, we first numerically calculate the transfer probability of a single phonon in the parameter space (δ, w) of the Gaussian modulation while the pumping duration $T = 50$ ms and the parameter $G_0 = 100$ Hz are kept fixed. The results are presented in Fig. 3(a), while a backward pumping (i.e., from oscillator 7 to oscillator 1) is also calculated and discussed in Supplemental Material [57]. We remark that these calculations go beyond the analytical results in Eq. (1) and indicate the richness of the phononic adiabatic pumping in finite SSH chains. In this Letter, we focus on the region $\delta > 0$. A close look at both the forward and the backward coherent transfer is presented in Fig. 3(b) for $w = 9$ ms. The results clearly demonstrate the nonreciprocity, i.e., $P_{1\to7} \neq P_{7\to1}$ due to time-reversal symmetry breaking. From these results, an excellent parameter for unidirectional coherent transfer is achieved at $\delta = 6.1$ ms when $w = 9$ ms.

Guided by the aforementioned calculation results, we engineer the six parametric voltages $V_{ac}^{ij}(t)$ to achieve the designed couplings and their dynamic modulations, as shown in Fig. 2(d). To test the unidirectional coherent transfer of phonons, we excite phonons in the first oscillator and then apply the designed dynamic modulations to the couplings. In the experimental regime, a huge number of phonons are generated and the number of phonons can be described by the classical vibration intensity $|x_1|^2$. This quantity for all oscillators was monitored via the lock-in amplifiers during the pumping process [44].

In Fig. 3(c), we present the measured normalized vibration intensity as a function of time and site index for $w = 9$ ms and $\delta = 6.1$ ms. The measured results agree fairly well with the simulation in Fig. 3(e) with the same parameters. An intriguing feature is that all the even sites are barely excited during the whole process. To clearly demonstrate the nonreciprocity of the adiabatic pumping, we also performed measurements for the setup with the initial phonons excited at the site 7. Results in Fig. 3(d) show that the backward propagation is suppressed, demonstrating clearly the nonreciprocal, unidirectional phonon

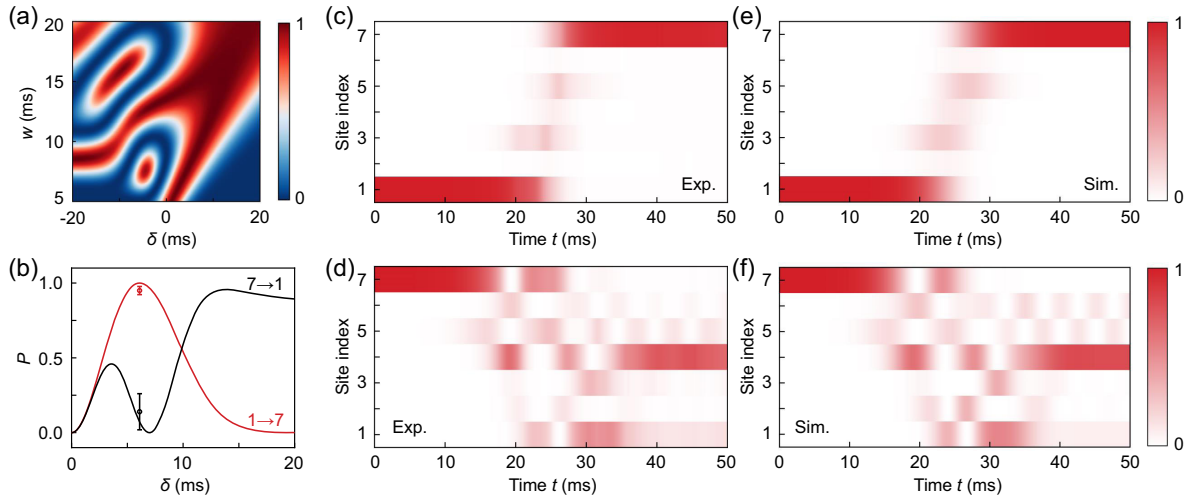

FIG. 3. Nonreciprocal adiabatic pumping of phonons. (a) Numerical result of the transfer probability $P_{1\to7}$ in parameter space (δ, w). (b) The forward transfer probability $P_{1\to7}$ and the backward transfer probability $P_{7\to1}$ for $w = 9$ ms. (c),(d) Experiment of forward and backward phonon transport for $w = 9$ ms and $\delta = 6.1$ ms, respectively. (e),(f) Simulation counterpart of (c),(d). Experimental results (c),(d) and numerical simulations (e),(f) are derived from the normalized vibration intensities and single phonon probability distributions.

transfer from site 1 to site 7. Again the measured results agree well with the simulation results in Fig. 3(f). The measured transfer probabilities $P_{1\to7}$ and $P_{7\to1}$ also agree with the calculated results in Fig. 3(b) where the standard error comes from statistics for many repeated measurements.

Robustness against noises.—We now verify the robustness of the adiabatic phonon transfer against noises in the electrical gate voltages that control the couplings between oscillators. In particular, we separately examine the effect of white noise and impulse noise on the transfer scheme. As shown in the inset of Fig. 4(b) and Supplemental Material [57], different Gaussian white noises with the same standard deviation σ are added into neighboring couplings g_i $(i = 1, \ldots, 6)$. Figure 4(a) presents the eigenenergy spectrum of the dynamically modulated topological insulator with $N = 7$ under the white noises. It is evident that the phonon transfer channel (topological zero state) $|\psi_0\rangle$ is still protected by the energy gap. Therefore, the transfer probability $P_{1\to7}$ keeps efficient with the increase of noise ratio σ/G_0, see Fig. 4(b). Each transfer probability of Fig. 4(b) is the statistical result under one hundred sets of random noises with Gaussian distribution.

For the experiments under impulse noises, we deliberately generate three types of square-wave pulses in the couplings [57]. Figure 4(c) gives the eigenenergy of the dynamic topological insulator under one of the impulse noises. The corresponding robustness results are shown in Fig. 4(d). The other two impulse noises and related experimental results are exhibited in Supplemental Material [57]. We find that this robustness holds even the strength of the impulse noises reach 30% of G_0. The error of data in Figs. 4(b) and 4(d) is primarily caused by the tiny variations of oscillators' frequencies when continuously varying the amplitudes of control voltages in the experiment. The robustness of unidirectional phonon transfer is also checked by numerical simulations in Supplemental Material [57].

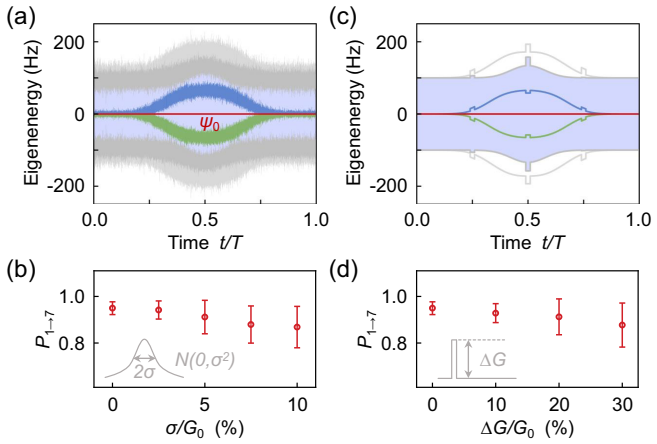

FIG. 4. Robustness against noises. (a),(c) Eigenenergy spectrums of the dynamically modulated topological insulator with $N = 7$ under the Gaussian white noises and the impulse noises, respectively. These noises are present at the control voltages, which is equivalent to the noises on the interactions g_i. The topological zero-energy eigenmode (the red line) is still protected by the energy gap represented by the blue region. (b),(d) The transfer probability $P_{1\to7}$ versus two kinds of noise ratio σ/G_0 and $\Delta G/G_0$. Insets: the magnitudes of the white noises and the impulse noises are described by the standard deviation σ of normal distributions and the amplitude ΔG of square-wave pulses, respectively. The duration time of each square-wave pulse is 1 ms. The transmission period $T = 50$ ms and the interaction $G_0 = 100$ Hz. Error bars represent the statistical confidence of 1 standard deviation.

Summary and outlook.—In conclusion, we realize the adiabatic pumping of phonons in a 1D nanomechanical topological insulator. The underlying scheme provides a way to achieve high fidelity unidirectional coherent transfer of phonons and is robust against noises. Our experiment unveils an excellent example where dynamic modulation can offer unprecedented control over phonons in nanomechanical systems and a remarkable way of achieving nonreciprocal phonon dynamics for future applications, such as cooling phononic resonators [9], chiral transport [64], and routing quantum information in phononic networks [65]. The dynamic modulation also opens a pathway toward temporal pumping [66–68], synthetic gauge fields [63], and on-chip topological phononic logic devices [69,70]. Moreover, although our experiment was carried out with coherent excitations, the topologically protected unidirectional transport is valid for transferring single quantum states [25]. This scheme could be expanded to other tunable quantum systems, including superconducting circuits and cold atoms systems.

The authors acknowledge the support of the National Key R&D Program of China (Grants No. 2021YFB3202800 and No. 2018YFA0306600), the National Natural Science Foundation of China (Grants No. 12125504 and No. 12074281), Anhui Initiative in Quantum Information Technologies (Grant No. AHY050000), China Postdoctoral Science Foundation (Grants No. 2021M693094 and No. 2021M693096), and the Fundamental Research Funds for the Central Universities. This work was partially carried out at the USTC Center for Micro and Nanoscale Research and Fabrication.

*zhoujw@ustc.edu.cn
†djf@ustc.edu.cn

[1] N. Rossi, F. R. Braakman, D. Cadeddu, D. Vasyukov, G. Tütüncüoglu, A. F. i. Morral, and M. Poggio, Nat. Nanotechnol. **12**, 150 (2017).
[2] L. M. de Lépinay, B. Pigeau, B. Besga, P. Vincent, P. Poncharal, and O. Arcizet, Nat. Nanotechnol. **12**, 156 (2017).
[3] S. R. Sklan, AIP Adv. **5**, 053302 (2015).
[4] H. Fu, Z.-c. Gong, L.-p. Yang, T.-h. Mao, C.-p. Sun, S. Yi, Y. Li, and G.-y. Cao, Phys. Rev. Appl. **9**, 054024 (2018).
[5] I. Mahboob and H. Yamaguchi, Nat. Nanotechnol. **3**, 275 (2008).
[6] I. Mahboob, E. Flurin, K. Nishiguchi, A. Fujiwara, and H. Yamaguchi, Nat. Commun., **2**, 198 (2011).
[7] P. Huang, L. Zhang, J. Zhou, T. Tian, P. Yin, C. Duan, and J. Du, Phys. Rev. Lett. **117**, 017701 (2016).
[8] S. Barzanjeh, M. Wulf, M. Peruzzo, M. Kalaee, P. B. Dieterle, O. Painter, and J. M. Fink, Nat. Commun. **8**, 953 (2017).
[9] H. Xu, L. Jiang, A. A. Clerk, and J. G. E. Harris, Nature (London) **568**, 65 (2019).
[10] L. M. de Lépinay, C. F. Ockeloen-Korppi, M. J. Woolley, and M. A. Sillanpää, Science **372**, 625 (2021).
[11] X. Ma, J. J. Viennot, S. Kotler, J. D. Teufel, and K. W. Lehnert, Nat. Phys. **17**, 322 (2021).
[12] J. Moser, A. Eichler, J. Güttinger, M. I. Dykman, and A. Bachtold, Nat. Nanotechnol. **9**, 1007 (2014).
[13] G. S. MacCabe, H. Ren, J. Luo, J. D. Cohen, H. Zhou, A. Sipahigil, M. Mirhosseini, and O. Painter, Science **370**, 840 (2020).
[14] D. Høj, F. Wang, W. Gao, U. B. Hoff, O. Sigmund, and U. L. Andersen, Nat. Commun. **12**, 5766 (2021).
[15] P.-B. Li, Z.-L. Xiang, P. Rabl, and F. Nori, Phys. Rev. Lett. **117**, 015502 (2016).
[16] M. Forsch, R. Stockill, A. Wallucks, I. Marinković, C. Gärtner, R. A. Norte, F. van Otten, A. Fiore, K. Srinivasan, and S. Gröblacher, Nat. Phys. **16**, 69 (2020).
[17] T. Faust, J. Rieger, M. J. Seitner, J. P. Kotthaus, and E. M. Weig, Nat. Phys. **9**, 485 (2013).
[18] H. Okamoto, A. Gourgout, C.-Y. Chang, K. Onomitsu, I. Mahboob, E. Y. Chang, and H. Yamaguchi, Nat. Phys. **9**, 480 (2013).
[19] M. J. Weaver, F. Buters, F. Luna, H. Eerkens, K. Heeck, S. de Man, and D. Bouwmeester, Nat. Commun. **8**, 824 (2017).
[20] Z.-Z. Zhang, X.-X. Song, G. Luo, Z.-J. Su, K.-L. Wang, G. Cao, H.-O. Li, M. Xiao, G.-C. Guo, L. Tian, G.-W. Deng, and G.-P. Guo, Proc. Natl. Acad. Sci. U.S.A. **117**, 5582 (2020).
[21] D. Hälg, T. Gisler, E. C. Langman, S. Misra, O. Zilberberg, A. Schliesser, C. L. Degen, and A. Eichler, Phys. Rev. Lett. **128**, 094301 (2022).
[22] H. Okamoto, R. Schilling, H. Schütz, V. Sudhir, D. J. Wilson, H. Yamaguchi, and T. J. Kippenberg, Appl. Phys. Lett. **108**, 153105 (2016).
[23] K. Gajo, S. Schüz, and E. M. Weig, Appl. Phys. Lett. **111**, 133109 (2017).
[24] Z.-C. Gong, H. Fu, T.-H. Mao, Q. Yuan, C.-Y. Shen, C.-P. Sun, Y. Li, and G.-Y. Cao, Appl. Phys. Lett. **118**, 203505 (2021).
[25] M. Christandl, N. Datta, A. Ekert, and A. J. Landahl, Phys. Rev. Lett. **92**, 187902 (2004).
[26] M. B. Plenio, J. Hartley, and J. Eisert, New J. Phys. **6**, 36 (2004).
[27] J. Zhang, G. L. Long, W. Zhang, Z. Deng, W. Liu, and Z. Lu, Phys. Rev. A **72**, 012331 (2005).
[28] R. J. Chapman, M. Santandrea, Z. Huang, G. Corrielli, A. Crespi, M.-H. Yung, R. Osellame, and A. Peruzzo, Nat. Commun. **7**, 11339 (2016).
[29] M. Bellec, G. M. Nikolopoulos, and S. Tzortzakis, Opt. Lett. **37**, 4504 (2012).
[30] A. Perez-Leija, R. Keil, A. Kay, H. Moya-Cessa, S. Nolte, L.-C. Kwek, B. M. Rodríguez-Lara, A. Szameit, and D. N. Christodoulides, Phys. Rev. A **87**, 012309 (2013).
[31] X. Li, Y. Ma, J. Han, T. Chen, Y. Xu, W. Cai, H. Wang, Y. P. Song, Z.-Y. Xue, Z.-q. Yin, and L. Sun, Phys. Rev. Appl. **10**, 054009 (2018).
[32] T. Tian, S. Lin, L. Zhang, P. Yin, P. Huang, C. Duan, L. Jiang, and J. Du, Phys. Rev. B **101**, 174303 (2020).
[33] Z. Yang, F. Gao, X. Shi, X. Lin, Z. Gao, Y. Chong, and B. Zhang, Phys. Rev. Lett. **114**, 114301 (2015).
[34] R. Süsstrunk and S. D. Huber, Science **349**, 47 (2015).

[35] S. D. Huber, Nat. Phys. **12**, 621 (2016).
[36] J. Cha, K. W. Kim, and C. Daraio, Nature (London) **564**, 229 (2018).
[37] M. Yan, J. Lu, F. Li, W. Deng, X. Huang, J. Ma, and Z. Liu, Nat. Mater. **17**, 993 (2018).
[38] G. Ma, M. Xiao, and C. T. Chan, Nat. Rev. Phys. **1**, 281 (2019).
[39] H. Ren, T. Shah, H. Pfeifer, C. Brendel, V. Peano, F. Marquardt, and O. Painter, arXiv:2009.06174.
[40] B. Xie, H.-X. Wang, X. Zhang, P. Zhan, J.-H. Jiang, M. Lu, and Y. Chen, Nat. Rev. Phys. **3**, 520 (2021).
[41] Y. Wu, M. Yan, Z.-K. Lin, H.-X. Wang, F. Li, and J.-H. Jiang, Sci. Bull. **66**, 1959 (2021).
[42] J. Ma, X. Xi, Y. Li, and X. Sun, Nat. Nanotechnol. **16**, 576 (2021).
[43] J. del Pino, J. J. Slim, and E. Verhagen, Nature (London) **606**, 82 (2022).
[44] T. Tian, Y. Ke, L. Zhang, S. Lin, Z. Shi, P. Huang, C. Lee, and J. Du, Phys. Rev. B **100**, 024310 (2019).
[45] A. Youssefi, S. Kono, A. Bancora, M. Chegnizadeh, J. Pan, T. Vovk, and T. J. Kippenberg, arXiv:2111.09133.
[46] M. J. Bereyhi, A. Arabmoheghi, A. Beccari, S. A. Fedorov, G. Huang, T. J. Kippenberg, and N. J. Engelsen, Phys. Rev. X **12**, 021036 (2022).
[47] N. Lang and H. P. Büchler, npj Quantum Inf. **3**, 47 (2017).
[48] F. Mei, G. Chen, L. Tian, S.-L. Zhu, and S. Jia, Phys. Rev. A **98**, 012331 (2018).
[49] S. Longhi, Phys. Rev. B **99**, 155150 (2019).
[50] Y.-X. Shen, L.-S. Zeng, Z.-G. Geng, D.-G. Zhao, Y.-G. Peng, and X.-F. Zhu, Phys. Rev. Appl. **14**, 014043 (2020).
[51] I. Brouzos, I. Kiorpelidis, F. K. Diakonos, and G. Theocharis, Phys. Rev. B **102**, 174312 (2020).
[52] J. Cao, W.-X. Cui, X. X. Yi, and H.-F. Wang, Phys. Rev. A **103**, 023504 (2021).
[53] N. E. Palaiodimopoulos, I. Brouzos, F. K. Diakonos, and G. Theocharis, Phys. Rev. A **103**, 052409 (2021).
[54] J. Yuan, C. Xu, H. Cai, and D.-W. Wang, APL Photonics **6**, 030803 (2021).
[55] W. P. Su, J. R. Schrieffer, and A. J. Heeger, Phys. Rev. Lett. **42**, 1698 (1979).
[56] J. K. Asbóth, L. Oroszlány, and A. Pályi, *A Short Course on Topological Insulators* (Springer International Publishing, New York, 2016).
[57] See Supplemental Material at http://link.aps.org/supplemental/10.1103/PhysRevLett.129.215901 for the approximate three-level description, transports in parameter spaces, dissipative even sites, experimental details, and robustness against noises.
[58] D. L. Sounas and A. Alù, Nat. Photonics **11**, 774 (2017).
[59] H. Nassar, B. Yousefzadeh, R. Fleury, M. Ruzzene, A. Alù, C. Daraio, A. N. Norris, G. Huang, and M. R. Haberman, Nat. Rev. Mater. **5**, 667 (2020).
[60] N. V. Vitanov, A. A. Rangelov, B. W. Shore, and K. Bergmann, Rev. Mod. Phys. **89**, 015006 (2017).
[61] S. Lin, L. Zhang, T. Tian, C.-K. Duan, and J. Du, Nano Lett. **21**, 1025 (2021).
[62] A. Cleland and M. Roukes, Sens. Actuators A **72**, 256 (1999).
[63] J. P. Mathew, J. del Pino, and E. Verhagen, Nat. Nanotechnol. **15**, 198 (2020).
[64] A. McDonald, T. Pereg-Barnea, and A. A. Clerk, Phys. Rev. X **8**, 041031 (2018).
[65] S. J. M. Habraken, K. Stannigel, M. D. Lukin, P. Zoller, and P. Rabl, New J. Phys. **14**, 115004 (2012).
[66] I. H. Grinberg, M. Lin, C. Harris, W. A. Benalcazar, C. W. Peterson, T. L. Hughes, and G. Bahl, Nat. Commun. **11**, 974 (2020).
[67] M. I. N. Rosa, R. K. Pal, J. R. F. Arruda, and M. Ruzzene, Phys. Rev. Lett. **123**, 034301 (2019).
[68] Y. Xia, E. Riva, M. I. N. Rosa, G. Cazzulani, A. Erturk, F. Braghin, and M. Ruzzene, Phys. Rev. Lett. **126**, 095501 (2021).
[69] R. Süsstrunk, P. Zimmermann, and S. D. Huber, New J. Phys. **19**, 015013 (2017).
[70] H. Pirie, S. Sadhuka, J. Wang, R. Andrei, and J. E. Hoffman, Phys. Rev. Lett. **128**, 015501 (2022).